Available online at www.sciencedirect.com
SCIENCE DIRECT
Bioorganic & Medicinal Chemistry Letters
Bioorganic & Medicinal Chemistry Letters 16 (2006) 1735–1739

Novel, potent P^2–P^3 pyrrolidine derivatives of ketoamide-based cathepsin K inhibitors

David G. Barrett,[a,†] John G. Catalano,[a,*] David N. Deaton,[a] Anne M. Hassell,[b] Stacey T. Long,[c] Aaron B. Miller,[b] Larry R. Miller,[d] John A. Ray,[a] Vicente Samano,[a] Lisa M. Shewchuk,[b] Kevin J. Wells-Knecht,[e,‡] Derril H. Willard, Jr.[f,§] and Lois L. Wright[g]

[a]*Department of Medicinal Chemistry, GlaxoSmithKline, Research Triangle Park, NC 27709, USA*
[b]*Discovery Research Computational, Analytical, and Structural Sciences, GlaxoSmithKline, Research Triangle Park, NC 27709, USA*
[c]*Department of World Wide Physical Properties, GlaxoSmithKline, Research Triangle Park, NC 27709, USA*
[d]*Department of Molecular Pharmacology, GlaxoSmithKline, Research Triangle Park, NC 27709, USA*
[e]*Department of Research Bioanalysis and Drug Metabolism, GlaxoSmithKline, Research Triangle Park, NC 27709, USA*
[f]*Department of Gene Expression and Protein Purification, GlaxoSmithKline, Research Triangle Park, NC 27709, USA*
[g]*Discovery Research Biology, GlaxoSmithKline, Research Triangle Park, NC 27709, USA*

Received 26 October 2005; revised 29 November 2005; accepted 30 November 2005
Available online 11 January 2006

Abstract—Starting from a potent pantolactone ketoamide cathepsin K inhibitor discovered from structural screening, conversion of the lactone scaffold to a pyrrolidine scaffold allowed exploration of the S^3 subsite of cathepsin K. Manipulation of P^3 and $P^{1'}$ groups afforded potent inhibitors with drug-like properties.

Continual structural remodeling of skeletal tissue is necessary to maintain strong healthy bone. Osteoclasts and osteoblasts are specialized cells that affect remodeling through an integrated process of bone resorption and bone formation.[1] Bone density and structural integrity deteriorate when this remodeling begins to favor bone resorption over bone formation, resulting in susceptibility to fracture. Osteoclasts utilize secreted acid and proteolytic enzymes to degrade the mineral and matrix components of bone, respectively. The main proteolytic enzyme secreted is cathepsin K, a cysteine protease which hydrolyzes type I collagen, the primary constituent of bone matrix.[2] Small molecule inhibitors of cathepsin K have proven efficacious in attenuating bone resorption in humans,[3] as well as in animal models of osteoporosis.[4]

This group has previously reported potent α-ketoamide inhibitors of cathepsin K.[5–9] The P^2 pantolactone moiety of ketoamide **1** ($IC_{50} = 3.0$ nM) was discovered through structural screening of the available chemical directory (ACD) as part of an ongoing structure/activity relationship analysis.[10] Although quite potent, inhibitor **1** exhibited poor pharmacokinetic (PK) properties in rats with a low terminal half-life and no oral bioavailability. Poor PK parameters were presumably due, at least in part, to the observed instability of the lactone in plasma. A second liability of the pantolactone moiety was the lack of suitable functionality for rapid diversification. In order to overcome the PK liabilities of pantolactone **1**, and also to facilitate SAR progression, a plasma-stable P^2 substituent readily amenable to derivatization was sought. Reasoning that the geminal dimethyl substituted pyrrolidine P^2 moiety of **2** would be equally effective in filling the hydrophobic S^2 binding pocket of the enzyme, without the instability observed with the pantolactone, a synthetic route to the pyrrolidine functionality was developed. The nucleophilic

Keywords: Cathepsin K; Inhibitor; Osteoporosis; Ketoamide; Synthesis.
* Corresponding author. Tel.: +1 919 483 6264; e-mail: john.g.catalano@gsk.com
† Present address: Lilly Forschung GmbH, Essener Str. 93, 22419 Hamburg, Germany.
‡ Present address: Schering-Plough Research Institute, 2015 Galloping Hill, Kenilworth, NJ 07033, USA.
§ Deceased.

0960-894X/$ - see front matter © 2005 Elsevier Ltd. All rights reserved.
doi:10.1016/j.bmcl.2005.11.101

nitrogen of the pyrrolidine also offered a handle for ready substitution.

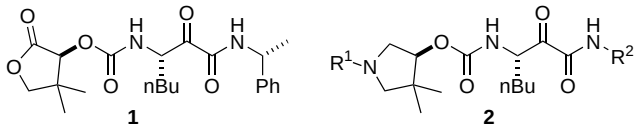

The synthesis of inhibitors **2a**–**2y** is represented in Scheme 1. (*S*)-(+)-Pantolactone **3** was reduced with sodium borohydride and the resulting triol **4** treated with methanesulfonyl chloride to afford the disulfonate **5**. Treatment of **5** with benzylamine afforded the cyclized pyrrolidinol **6**. The chloroformate formed by treating **6** with phosgene was coupled with known amino alcohols **7a**[7] or **7b**[9] to give a carbamate, which after the removal of the benzyl-protecting group afforded the amines **8a**–**8b**. The resulting pyrrolidines **8a**–**8b** were combined with a variety of acid chlorides, chloroformates, isocyanates, and sulfonyl chlorides to obtain amides, carbamates, ureas, and sulfonamides, respectively. The α-hydroxy amides were then oxidized with Dess–Martin periodinane to afford α-ketoamides **2a**–**2y**.

Inhibitor **2z** was synthesized via mixed carbonate **12** as shown in Scheme 2. Pyrrolidinol **6** was deprotected via acidic hydrogenolysis to give pyrrolidine **9**, which was coupled with 2-chlorobenzothiazole **10** to give the substituted pyrrolidinol **11**. Treatment of **11** with 4-nitrophenylchloroformate gave the mixed carbonate **12**, which was then coupled with the amino alcohol **7b**. Dess–Martin oxidation of the α-hydroxyamide then yielded the ketoamide **2z**.

Inhibitor **2aa** was synthesized similarly to **2z** via the mixed carbonate **16** as shown in Scheme 3. First, commercially available 5-(trifluoromethyl)-1,3,4-thiadiazol-2-amine **13** was converted to the bromide **14** via diazotization. Then, the bromide **14** was coupled with the pyrrolidinol **9** to give the substituted pyrrolidinol **15**. Finally, after the carbonate **16** was formed by treating pyrrolidinol **15** with 4-nitrophenylchloroformate, it

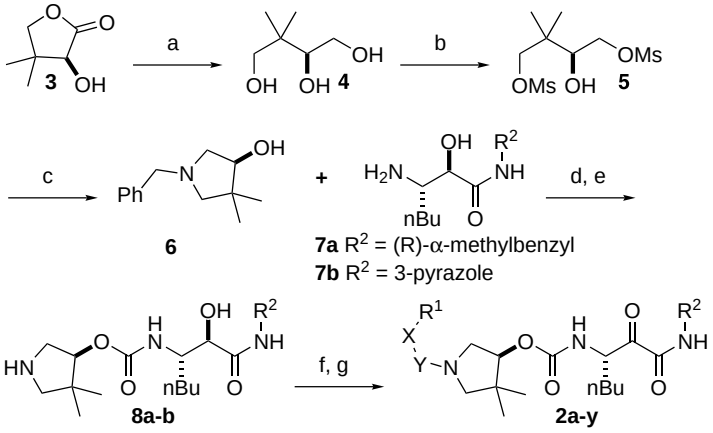

Scheme 1. Reagents and conditions: (a) $NaBH_4$, MeOH, 0 °C to rt, 99%; (b) MsCl, pyridine, 0 °C to rt, 52%; (c) benzylamine, EtOH, 120 °C, sealed tube, 90%; (d) **6**, 1.93 M phosgene in toluene, pyridine, CH_2Cl_2, 0 °C to rt; then **7a** or **7b**, Et_3N, THF, 41%; (e) H_2, 10% Pd/C, EtOH, 75%; (f) R^1COCl or R^1OCOCl or $R^1N{=}C{=}O$ or R^1SO_2Cl; (g) Dess–Martin periodinane, CH_2Cl_2, 27–96% (2 steps).

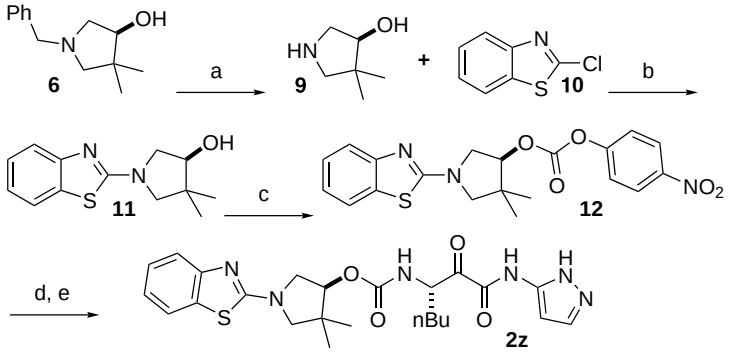

Scheme 2. Reagents: (a) H_2, 10% Pd/C, 1 M HCl (aq), EtOH, 99%; (b) **10**, $NaHCO_3$, *i*-PrOH, H_2O, 96%; (c) 4-nitrophenylchloroformate, pyridine, CH_2Cl_2, 73%; (d) **7b**, iPr_2NEt, DMF, 77%; (e) Dess–Martin periodinane, CH_2Cl_2, 67%.

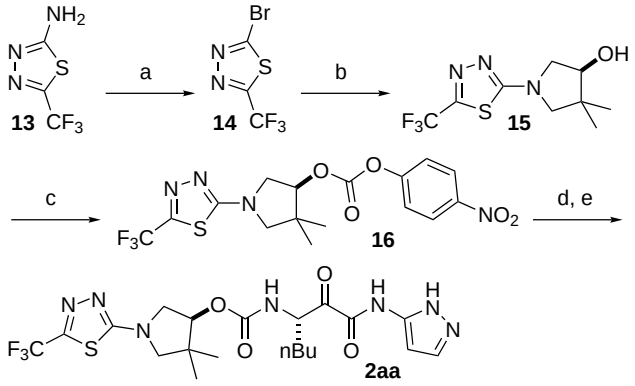

Scheme 3. (a) HBr, Br_2, $NaNO_2$, NaOH (aq), 54%; (b) **9**, iPr_2NEt, isopropanol, reflux, 88%; (c) 4-nitrophenylchloroformate, pyridine, CH_2Cl_2; (d) **7b**, iPr_2NEt, DMF, 21% (2 steps); (e) Dess–Martin periodinane, CH_2Cl_2, 84%.

was coupled to amine **7b** and oxidized to provide the ketoamide **2aa**.

An initial set of analogs **2a**–**2l** was synthesized to investigate both the linker and spatial requirements for the P^2–P^3 substituent. A phenyl group was extended 2, 3, 4, or 5 bond lengths from the pyrrolidine core and attached via an amide, carbamate, urea, or sulfonamide linker. As shown in Table 1, the urea analogs **2f**, **2i**, and **2l** (IC_{50}s = 3.8–6.6 nM) were amongst the more potent inhibitors of the initial set and their potencies did not show a significant dependence on the chain length between the pyrrolidine nitrogen and the phenyl substituent. The potencies of the carbamate derivatives **2e**, **2h**, and **2k** (IC_{50}s = 24–32 nM) were also not appreciably affected by chain length, but these analogs were ~5-fold less potent than the corresponding urea derivatives. In contrast, the activity of analogous amide derivatives **2d** (IC_{50} = 3.0 nM) and **2j** (IC_{50} = 27 nM) was much more dependent on the chain length. Sulfonamide **2g** (IC_{50} = 17 nM) was roughly 5-fold less potent than its analogous amide **2d**. Although phenylamide **2b** (IC_{50} = 65 nM) was the least potent of the series, larger aryl and heteroaryl amides **2o**–**2r** (IC_{50}s = 1.6–6.9 nM) were quite potent. These larger aryl amides may act as conformationally restricted analogs of **2d** and were indeed equipotent. Similarly, carbamate **2s** (IC_{50} = 58 nM) is a conformationally restricted analog that shows similar potency to the unrestricted analog **2h**. Carbamate analogs **2t** (IC_{50} = 5.0 nM) and **2u** (IC_{50} = 2.1 nM) include a 4-biphenyl substituent that further extends the phenyl group toward P^3 in a conformationally restricted manner. These carbamate inhibitors showed significantly improved potencies compared to those of other carbamate derivatives. Biphenyl amide **2r** (IC_{50} = 6.9 nM) also exhibited good potency, but was larger and no more potent than **2d**.

Inhibitors of this series generally exhibited excellent selectivity against the exopeptidases cathepsin B and cathepsin H, as well as against the endopeptidase cathepsin L, as shown in Table 1. In fact, most of the inhibitors were greater than 1000-fold selective and only a few were less than 100-fold selective versus these cathepsins. However, these inhibitors were much less selective against the closely related endopeptidase cathepsins S and V.

Inhibitors **2b**–**2y** were significantly less potent against rat cathepsin K than against the human isoform. Although rat cathepsin K functions similarly to human cathepsin K in respect to bone resorption activity, there are significant structural differences in the active sites of rat and human cathepsin K.[2] Indeed, the lack of potency of such inhibitors versus rat cathepsin K has hampered efforts to progress inhibitors via rodent-based assays such as the ex vivo rat calvarial resorption assay[11,12] and the thyroid-parathyroidectomized hypocalcemic (TPTX) rat assay.[13]

An X-ray co-crystal structure of cathepsin K with inhibitor **2x** (Table 2) is shown in Figure 1. As with previously solved X-ray co-crystal structures of cathepsin K and ketoamide inhibitors,[5,8,9] a covalent hemithioketal intermediate is formed between the ^{25}Cys of the enzyme and the α-keto moiety of the inhibitor. The oxyanion hole is occupied by the carbonyl of the amide rather than the hemithioketal hydroxyl group. As predicted, the geminal dimethyl substitution of the pyrrolidine inhibitors effectively fills the S^2 pocket of the enzyme. Unlike our previously reported ketoamide inhibitors, however, this inhibitor does not extend toward the S^3 subsite of the enzyme. Rather, the P^3 substitution attached to the pyrrolidine nitrogen extends into solvent, possibly explaining the similar potency of linker extended P^3 analogs in the urea series. A hydrogen bond between ^{161}Asn and the $P^{1'}$ amide nitrogen is accomplished via a bridging water molecule (red sphere).

Compounds **2c**, **2d**, and **2i** were potent examples of the sulfonamide, amide, and urea classes, respectively, and were therefore chosen for progression into PK studies (Table 2). Amide derivative **2d** exhibited very good permeability (P_{APP} = 410 nm/s) as measured in a Madin–Darby canine kidney (MDCK) permeability model as well as moderate solubility (0.068 mg/mL) as measured in fasted state-simulated intestinal fluid (FS-SIF). The oral bioavailability of **2d** (F = 29%) was similar that of urea analog **2i** (F = 21%), which had lower permeability (P_{APP} = 210 nm/s) and slightly lower solubility (FS-SIF = 0.053 mg/mL). Sulfonamide **2c** had a longer half-life and comparable oral bioavailability (F = 25%) to **2d** and **2i**, although permeability and solubility were not measured. All three inhibitors exhibited good volumes of distribution, moderate clearances, and relatively short half-lives in male Han Wistar rats. Inhibitors **2v**, **2w**, and **2x** were slightly less potent than **2d**, but incorporated heterocyclic ring substitution in an attempt to improve solubility and oral bioavailability. Despite similar permeability and solubility properties, the isoxazole analog **2v** was less orally bioavailable (F = 8.6%) than **2d** and had a shorter half-life with a lower volume of distribution. The basic pyridyl derivative **2w** exhibited an apparently longer half-life than **2d** and was slightly more soluble, which may contribute to the greater oral bioavailability (F = 45%) observed for this inhibitor.

Table 1. Inhibition of human cathepsin K and selectivity ratios versus other cathepsins

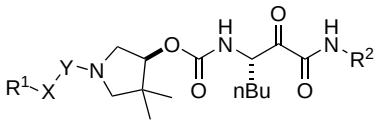

Compound	R^1	X	Y	R^2	Cat K IC_{50}[a] (nM)	rK/hK	B/K[b]	H/K[c]	L/K[d]	S/K[e]	V/K[f]
1					3.0	—	>500	>500	410	13	79
2a	Ph	—	CH_2	(R)-CH(Me)Ph	21	—	—	—	—	—	—
2b	Ph	—	CO	(R)-CH(Me)Ph	65	470	3800	—	370	43	110
2c	Ph	—	SO_2	(R)-CH(Me)Ph	8.3	110	7100	>13,000	74	16	79
2d	Ph	CH_2	CO	(R)-CH(Me)Ph	3.0	160	4300	>13,000	76	17	140
2e	Ph	O	CO	(R)-CH(Me)Ph	29	—	—	—	—	—	—
2f	Ph	NH	CO	(R)-CH(Me)Ph	4.3	890	2900	>13,000	1400	45	120
2g	Ph	CH_2	SO_2	(R)-CH(Me)Ph	17	490	5200	>13,000	910	12	79
2h	$PhCH_2$	O	CO	(R)-CH(Me)Ph	24	—	>10,000	>10,000	1300	83	170
2i	$PhCH_2$	NH	CO	(R)-CH(Me)Ph	3.8	870	4600	>13,000	1200	46	130
2j	$Ph(CH_2)_2$	CH_2	CO	(R)-CH(Me)Ph	27	—	—	—	—	—	—
2k	$Ph(CH_2)_2$	O	CO	(R)-CH(Me)Ph	32	—	—	—	—	—	—
2l	$Ph(CH_2)_2$	NH	CO	(R)-CH(Me)Ph	6.6	930	5200	>13,000	760	26	85
2m	1-Morpholine	—	CO	(R)-CH(Me)Ph	16	76	210	>800	81	2.8	15
2n	4-Trifluoromethylphenyl	NH	CO	(R)-CH(Me)Ph	2.1	>120	>120	>120	>120	11	43
2o	2-Naphthalene	—	CO	(R)-CH(Me)Ph	1.6	510	760	>7900	890	62	56
2p	2-Benzothiophene	—	CO	(R)-CH(Me)Ph	2.8	430	540	>4500	1000	16	56
2q	5-Indole	—	CO	(R)-CH(Me)Ph	1.7	290	450	>7200	490	21	81
2r	4-Biphenyl	—	CO	(R)-CH(Me)Ph	6.9	54	250	>1800	320	5.8	8.7
2s	2-Naphthalene	O	CO	(R)-CH(Me)Ph	58	—	—	—	—	—	—
2t	4-Biphenyl	O	CO	(R)-CH(Me)Ph	5.0	240	650	>2500	200	13	42
2u	4-Biphenyl-CH_2	O	CO	(R)-CH(Me)Ph	2.1	430	100	>6000	960	9.1	81
2v	5-Isoxazolyl	—	CO	(R)-CH(Me)Ph	8.9	79	360	>1400	130	3.2	11
2w	3-Pyridyl	—	CO	(R)-CH(Me)Ph	14	55	360	>890	52	3.7	11
2x	3,5-Dimethyl-isoxazolyl	NH	CO	(R)-CH(Me)Ph	15	42	270	>810	39	2.6	9.1
2y	4-Trifluoromethylphenyl	NH	CO	3-Pyrazole	0.42	240	>600	>600	>600	6.7	36
2z	2-Benzthiazolyl	—	CO	3-Pyrazole	0.81	—	>310	>310	>310	6.6	32
2aa	5-CF_3-1,3,4-thiadiazolyl	—	CO	3-Pyrazole	1.0	—	>250	>250	>250	17	36

[a] Inhibition of recombinant human cathepsin K activity in a fluorescence assay using 400 pM cathepsin K with 10 μM Cbz-Phe-Arg-AMC as substrate in 100 mM NaOAc, 10 mM DTT, and 120 mM NaCl, pH 5.5. The IC_{50} values are means of two or three inhibition assays, individual data points in each experiment were within a 3-fold range of each other.

[b] B/K = IC_{50} against cathepsin B/IC_{50} against cathepsin K. Inhibition of recombinant human cathepsin B activity in a fluorescence assay using 250 pM cathepsin B with 10 μM Cbz-Phe-Arg-AMC as substrate in 100 mM NaOAc, 10 mM DTT, and 120 mM NaCl, pH 5.5.

[c] H/K = IC_{50} against cathepsin H/IC_{50} against cathepsin K. Inhibition of recombinant human cathepsin H activity in a fluorescence assay using 107 nM cathepsin H with 50 μM L-Arg-β-naphthalamide as substrate in 100 mM NaOAc, 10 mM DTT, and 120 mM NaCl, pH 5.5.

[d] L/K = IC_{50} against cathepsin L/IC_{50} against cathepsin K. Inhibition of recombinant human cathepsin L activity in a fluorescence assay using 300 pM cathepsin L with 5 μM Cbz-Phe-Arg-AMC as substrate in 100 mM NaOAc, 10 mM DTT, and 120 mM NaCl, pH 5.5.

[e] S/K = IC_{50} against cathepsin S/IC_{50} against cathepsin K. Inhibition of recombinant human cathepsin S activity in a fluorescence assay using 400 pM cathepsin S with 10 μM Cbz-Val-Val-Arg-AMC as substrate in 100 mM NaOAc, 10 mM DTT, and 120 mM NaCl, pH 5.5.

[f] V/K = IC_{50} against cathepsin V/IC_{50} against cathepsin K. Inhibition of recombinant human cathepsin V activity in a fluorescence assay using 150 pM cathepsin V with 2 μM Cbz-Phe-Arg-AMC as substrate in 100 mM NaOAc, 10 mM DTT, and 120 mM NaCl, pH 5.5.

Table 2. Pharmacokinetics of cathepsin K inhibitors

Compound	MDCK P_{APP} (nm/s)	Sol. FS-SIF[a] (mg/mL)	$t_{1/2}$[b] (min)	C_l[c] (mL/min/kg)	V_{SS}[d] (mL/kg)	F[e] (%)
1	—	0.240	11	460	3400	0.0
2c	—	—	150	27	2100	25
2d	410	0.068	63	26	1500	29
2i	210	0.053	61	32	1400	21
2v	480	0.068	36	18	500	8.6
2w	210	0.085	94	34	550	45
2x	12	0.320	35	83	1400	8.8
2y	18	0.14	75	77	2600	26
2z	250	0.160	180	65	2200	14
2aa	120	—	81	79	3300	13

[a] FS-SIF is the equilibrium solubility in fasted state-simulated intestinal fluid at pH = 6.8. The values are means of two measurements.

[b] $t_{1/2}$ is the iv terminal half-life dosed as a solution in male Han Wistar rats. All in vivo pharmacokinetic values are means of two experiments.

[c] C_l is the total clearance.

[d] V_{SS} is the steady-state volume of distribution.

[e] F is the oral bioavailability.

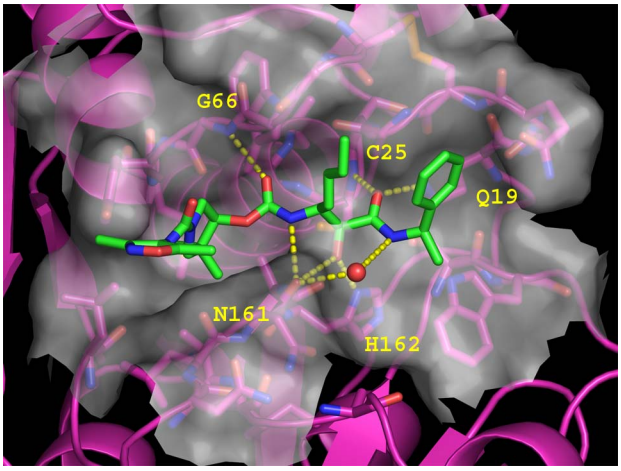

Figure 1. Active site of the X-ray co-crystal structure of compound **2x** complexed with cathepsin K. The cathepsin K carbons are colored magenta with inhibitor **2x** carbons colored green. The semi-transparent white surface represents the molecular surface, while hydrogen bonds are depicted as yellow dashed lines. The red sphere is a water molecule. The coordinates have been deposited in the Brookhaven Protein Data Bank, Accession No. 2BDL. This figure was generated using PYMOL version 0.97 (Delano Scientific, www.pymol.org).

Isoxazole analog **2x** was very soluble (FS-SIF = 0.320 mg/mL), but suffered from low permeability (P_{APP} = 12 nm/s), which may contribute to the low oral bioavailability (F = 8.8%) observed for this compound. Compounds **2y**, **2z**, and **2aa** incorporated a pyrazole at $P^{1'}$, which has been shown to impart improved potency, solubility, and oral bioavailability in previously studied series[8] These compounds were indeed the most potent of the current series and were quite soluble. Unfortunately, an improvement in oral bioavailability was not realized. In general, this entire series exhibited moderate to high clearances, relatively short half-lives, and moderate to good oral bioavailabilities.

In conclusion, this report summarizes the progression of P^2–P^3 pyrrolidine ketoamide-based cathepsin K inhibitors that were derived from a P^2 pantolactone lead structure. Potent inhibitors of cathepsin K with moderate PK were obtained. A co-crystal structure of an inhibitor bound to cathepsin K suggests that substitution of the pyrrolidine nitrogen is not optimal to interact with the S^3 subsite.

References and notes

1. Einhorn, T. A. In *Osteoporosis*; Marcus, R., Feldman, D., Kelsey, J., Eds.; Academic Press, Inc: San Diego, California, 1996; pp 3–22.
2. Deaton, D. N.; Kumar, S. *Prog. Med. Chem.* **2004**, *42*, 245.
3. Roy, S. K.; Pillai, G.; Woodworth, T.G.; Skerjanec, A.; Collins W.C.J. Presented at the 27th Annual Meeting of the American Society for Bone and Mineral Research (ASBMR), Nashville, Tennessee, USA, Sep. 23–27, 2005; Abstract 447.;
4. Stroup, G. B.; Lark, M. W.; Veber, D. F.; Bhattacharyya, A.; Blake, S.; Dare, L. C.; Erhard, K. F.; Hoffman, S. J.; James, I. E.; Marquis, R. W.; Ru, Y.; Vasko-Moser, J. A.; Smith, B. R.; Tomaszek, T.; Gowen, M. *J. Bone Miner. Res.* **2001**, *16*, 1739.
5. Barrett, D. G.; Catalano, J. G.; Deaton, D. N.; Hassell, A. M.; Long, S. T.; Miller, A. B.; Miller, L. R.; Shewchuk, L. M.; Wells-Knecht, K. J.; Willard, D. H., Jr.; Wright, L. L. *Bioorg. Med. Chem. Lett.* **2004**, *14*, 4897.
6. Barrett, D. G.; Catalano, J. G.; Deaton, D. N.; Long, S. T.; Miller, L. R.; Tavares, F. X.; Wells-Knecht, K. J.; Wright, L. L.; Zhou, H.-Q. Q. *Bioorg. Med. Chem. Lett.* **2004**, *14*, 2543.
7. Catalano, J. G.; Deaton, D. N.; Long, S. T.; McFadyen, R. B.; Miller, L. R.; Payne, J. A.; Wells-Knecht, K. J.; Wright, L. L. *Bioorg. Med. Chem. Lett.* **2004**, *14*, 719.
8. Tavares, F. X.; Boncek, V.; Deaton, D. N.; Hassell, A. M.; Long, S. T.; Miller, A. B.; Payne, A. A.; Miller, L. R.; Shewchuk, L. M.; Wells-Knecht, K.; Willard, D. H., Jr.; Wright, L. L.; Zhou, H.-Q. *J. Med. Chem.* **2004**, *47*, 588.
9. Barrett, D. G.; Boncek, V. M.; Catalano, J. G.; Deaton, D. N.; Hassell, A. M.; Jurgensen, C. H.; Long, S. T.; McFadyen, R. B.; Miller, A. B.; Miller, L. R.; Payne, J. A.; Ray, J. A.; Samano, V.; Shewchuk, L. M.; Tavares, F. X.; Wells-Knecht, K. J.; Willard, D. H.; Wright, L. L.; Zhou, H.-Q. Q. *Bioorg. Med. Chem. Lett.* **2005**, *15*, 3540.
10. Barrett, D. G.; Catalano, J. G.; Deaton, D. N.; Long, S. T.; McFadyen, R. B.; Miller, A. B.; Miller, L. R.; Wells-Knecht, K. J.; Wright, L. L. *Bioorg. Med. Chem. Lett.* **2005**, *15*, 2209.
11. Hahn, T. J.; Westbrook, S. L.; Halstead, L. R. *Endocrinology* **1984**, *114*, 1864.
12. Conaway, H. H.; Grigorie, D.; Lerner, U. H. *J. Endocrinol.* **1997**, *155*, 513.
13. Thompson, D. D.; Seedor, J. G.; Fisher, J. E.; Rosenblatt, M.; Rodan, G. A. *Proc. Natl. Acad. Sci. U.S.A.* **1988**, *85*, 5673.